Neutron dosimetry in solid water phantom

Cite as: AIP Conference Proceedings **1626**, 114 (2014); https://doi.org/10.1063/1.4901372
Published Online: 17 February 2015

Jorge Luis Benites-Rengifo, and Hector Rene Vega-Carrillo

Neutron Dosimetry in Solid Water Phantom

Jorge Luis Benites-Rengifo[1, 2, a)] and Hector Rene Vega-Carrillo[3, b)]

[1]*Centro Estatal de Cancerologia de Nayarit, Calzada de la Cruz 118 Sur, Tepic Nayarit, Mexico.*
[2]*Instituto Tecnico Superior de Radiologia, ITEC, Calle Leon 129, Tepic Nayarit, Mexico.*
[3]*Universidad Autonoma de Zacatecas, Unidad Academica de Estudios Nucleares, Apdo. postal 336, 98000, Zacatecas, Zac., Mexico.*

[a)] Corresponding author: jlbenitesr@prodigy.net.mx.
[b)]fermineutron@yahoo.com.

Abstract. The neutron spectra, the Kerma and the absorbed dose due to neutrons were estimated along the incoming beam in a solid water phantom. Calculations were carried out with the MCNP5 code, where the bunker, the phantom and the model of the15 MV LINAC head were modeled. As the incoming beam goes into the phantom the neutron spectrum is modified and the dosimetric values are reduced.

INTRODUCTION

In conformal radiotherapy treatments megavoltage X-rays and electrons beams are used to deliver a dose in the patient´s target volume. The photon or the electron beam is produced in a linear accelerator (LINAC); when the voltage is larger than 10 MV undesirable neutrons are induced. Neutrons have a high radiobiological efficiency and represent a risk for the patients. Also, neutrons induce activation of Ar and N in the air producing ^{41}Ar and ^{13}N, as well as in the components of the linac head and materials in the treatment room [1-4]. During the transport in the patient body neutrons are moderated and eventually thermalized. The aim of this work was to estimate the neutrons spectra, the Kerma and the absorbed dose in a solid water phantom using Monte Carlo methods with the MCNP5 code [5].

MATERIALS AND METHODS

The Cancer center of Nayarit has a 15 MV LINAC, this facility was modeled with the MCNP5 code. In the model, the bunker, the linac head, and a solid water phantom were included. The phantom was a regular parallelepiped of 30 x 100 x 30 cm^3 whose elemental composition is 8.1% H, 67.2% C, 2.4% N, 19.9% O_2, 0.1% Cl, 2.3% Ca, and its density is 1.02 g/cm^3 [6]. In the simulation, the phantom was located at the treatment position. The isocenter (IC) was 5 cm-deep in the phantom. Inside the phantom, several 0.9 cm-radius spherical cells were distributed along the length (Y-axis), width (X-axis) and depth (Z-axis) to estimate the spectra, the Kerma and the absorbed dose due to neutrons. Along Z-axis another cell was allocated 1-cm above the phantom surface (beam entrance surface). In the IC plane a point-like detector was modeled at 100 cm from the IC.

RESULTS

In Fig. 1 the neutron spectra, along the incoming beam, in the IC and outside the phantom (1 cm above the entrance surface) are shown; in this figure is also included the neutron spectrum at 100 cm from the IC.

In the incoming beam (outside the phantom) the neutron spectrum has evaporation, and epithermal and thermal neutrons. The largest component is the evaporation neutrons produced in the head. Also, there is a small contribution of epithermal and thermal neutrons that are backscattered from the phantom. As neutrons reach the IC, thermal neutrons become the largest component and the evaporation neutrons are strongly reduced due to neutron

XIII Mexican Symposium on Medical Physics
AIP Conf. Proc. 1626, 114-116 (2014); doi: 10.1063/1.4901372

moderation in the phantom. At 100 cm from the IC the spectrum contains uncollided, scattered and room-return neutrons [7]; here, the evaporation neutrons are shifted to lower energies. These features are the evidence that the patient body modifies the neutron spectrum and the part of the neutron energy is delivered to the patient body.

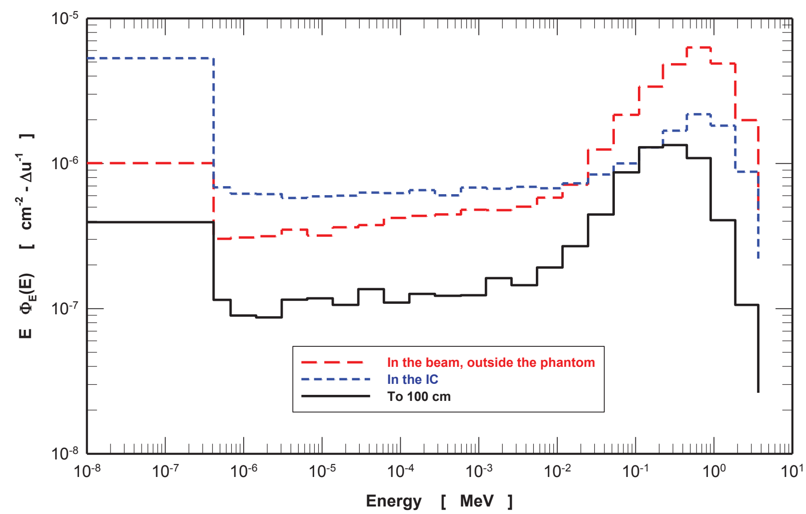

FIGURE 1. Neutron spectrum in IC and two points outside of phantom

In Fig. 2 the neutron spectra in the cells allocated along the Z-axis are shown. As the neutron beam penetrates the phantom the amount of neutrons decreases.

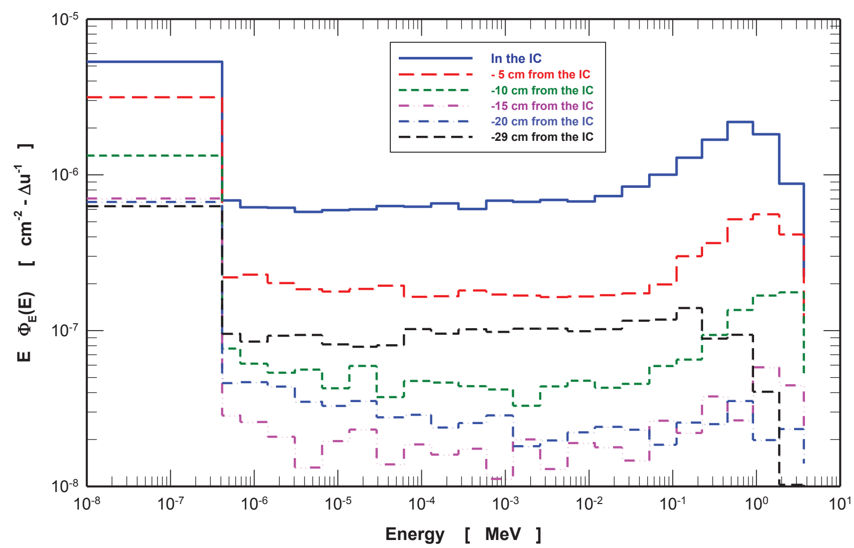

FIGURE 2. Calculated neutron spectra along the Z axis in the phantom

The amount of evaporation neutrons is reduced while the amount of thermal neutrons is increased due the elastic and inelastic interactions with the nuclei in the phantom. In the cell allocated at 29 cm in the Z axis, which is 1 cm measured from the back of the phantom, the amount of high energy neutrons is significantly reduced; in this spectrum mostly of the neutrons are epithermal and thermal. During a treatment this neutron spectrum will be reaching the patient´s spine.

The Kerma and absorbed dose, due to neutrons, in solid water are shown in Fig. 3. Along the Z-axis both values coincide meaning that there is electronic equilibrium in the cells, except in the detector sited in the back of the phantom, this is consistent with the effect noticed in the calculated neutron spectra.

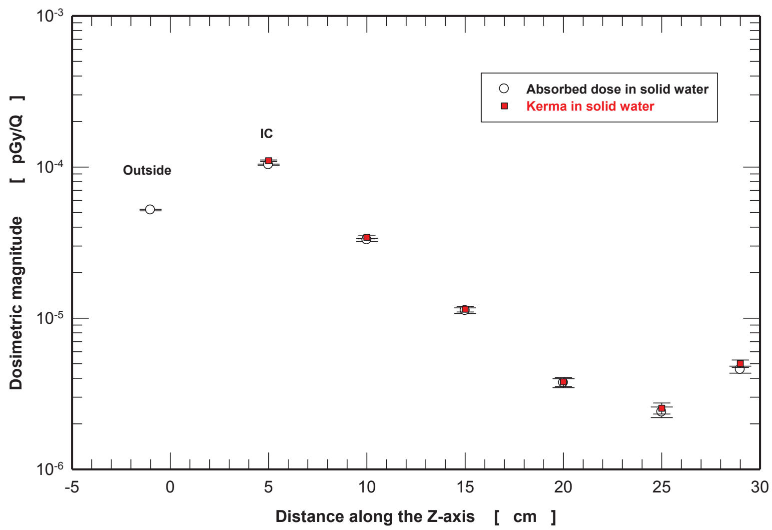

FIGURE 3. Calculated dosimetric magnitudes along the phantom Z axis
(pGy/Q is absorbed dose per neutron emitted by the linac, Q is the strength of the source term)

CONCLUSIONS

Using Monte Carlo methods the neutron spectra, the Kerma and neutron absorbed dose were estimated along the Z-axis in a solid water phantom. During a cancer treatment with a LINAC the photon beam is well collimated avoiding the healthy tissues; however the photoneutrons are distributed along the patient body and the neutron spectra are changed during the neutron interactions with the phantom. In the Z-axis there is electronic equilibrium in all the cells allocated along the incoming beam, except in the detector in the phantom rear where the high energy neutrons are strongly reduced.

ACKNOWLEDGEMENTS

The first author thanks to CONACyT for the scholarship to get the PhD degree.

REFERENCES

1. J. B. Awotwi-Pratt and N. M. Spyrou, J. Radioanal. Nucl. Chem., **271**, 679-684 (2007).
2. NCRP, *Neutron Contamination from Medical Electron Accelerators*. NCRP Report No 79 (National Council on Radiation Protection and Measurements, Bethesda, 1984), pp. 5-37.
3. H. R. Vega-Carrillo, E. Manzanares-Acuña, M.P. Iñiguez, E. Gallego and A. Lorente, (2007). Rad. Meas., **42**, 1373-1379 (2007).
4. J. H. Chao, W. S. Liu and C. Y. Chen, Rad. Meas., **42**, 1538-1544 (2007).
5. X-5 Monte Carlo Team. (2003). MCNP-A general Monte Carlo N-particle transport code. Version 5. LANL-UR-03-1987.
6. ICRU, *Tissue substitutes in radiation dosimetry and measurements*. ICRU Report 44 (International Commission on Radiation Units and Measurements, Bethesda, 1989), pp. 37-38.
7. H. R. Vega-Carrillo, E. Manzanares-Acuña, M. P. Iñiguez, E. Gallego and A. Lorente, Appl. Radiat. Isot., **42**, 413-419 2007.